Air speed control of airship-type fish robot

Kunihiko Sato* and Masafumi Uchida**

**The Graduate School of the University of Electro-Communications*
***The Department of Electronic Engineering, The University of Electro-Communications*
1-5-1, Chofugaoka, Chofu, Tokyo, Japan
(Tel: +81-42-443-5173; Fax: +81-42-443-5173)
(Email: sato@zidane.ee.uec.ac.jp)

Abstract: This paper deals with progress in the motion performance and control of a Balloon Fish Robot (BFR). The BFR is a fish-type airship robot that derives its propulsion from vibrations of two joints. The BFR is moved in three-dimensional space by an actuator. We consider the thrust of the BFR and measured it with a force sensor. The purpose of this research is to construct an equation of motion for the BFR and to control its air speed.

***Keywords*: Airship Robot, Fish Robot**

I. INTRODUCTION

Recently, there has been progress in research on airship robots that float in the air. An airship robot has the advantage of being able to move in three dimensions without being influenced by obstacles on the ground and without disturbing people's work. Moreover, because an airship uses a gas that is lighter than air to obtain buoyancy, the energy necessary for floatage is less than that of other types of flying robots, such as airplane and helicopter robots. Airship robots have been studies for applications in disaster relief and indoor patrol and surveillance systems [1].

On the other hand, there have been advances in research on the movement of fish, which have superior propulsive performance in water. There has been some work on applying fish-type underwater robots to offshore surveying and underwater surveys of natural resources [2][3]. In addition, a robot that employs the propulsion principle of aquatic organisms in the air, not water, has been developed. An example is the manta-type flying robot (Air Ray) developed by FESTO Co. developed.

We developed an airship robot based on a fish's propulsion principle, called the Balloon Fish Robot (BFR). The purpose of our research is to construct an equation of motion for the BFR and to control its air speed.

II. Structure and equation of motion of BFR

1. Structure of the BFR

Fig. 1 shows the structure of the BFR, and Fig. 2 shows a photograph of the BFR. The BFR is composed of three parts: the head, the body, and the caudal fin. The head and the body are formed of aluminum film balloons filled with helium, giving the BFR a buoyancy of about 300 grams.

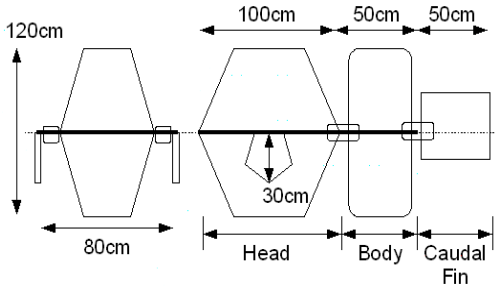

Fig.1. Structure of the BFR

Fig.2. Appearance of the BFR

The BFR has two joints. One is a servo motor-driven joint between the head and the body, and the other is a spring joint between the body and the caudal fin. The servo motor moves symmetrically by various angles and at various frequencies and the BFR vibrates smoothly to obtain thrust. This movement is generally referred to as a fish's wriggling motion [4].

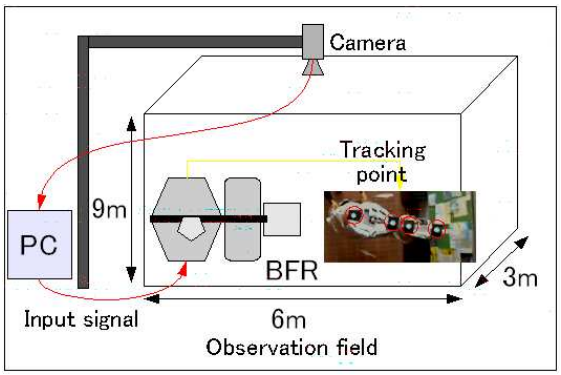

Fig.3. Real machine experimental system

2. Equation of motion of the BFR

Zhang constructed an equation of motion for an airship under the following three conditions [5]:

1. The airship is a rigid body.
2. There is no rotary motion about the three axes.
3. There is no air flow.

The propulsion direction of the BFR is taken as the x axis, the horizontal direction is taken as the y axis, and the vertical direction is taken as the z axis. Since we deal with propulsion of the BFR, it is assumed that there is no movement along the z axis. Because the wriggling motion is a symmetric motion, the y-axis components of the thrust cancel each other out. The x-axis component of the thrust determines the propulsion of the BFR. The equation of motion in the x-axis:

$$m\frac{d^2}{dt^2}x = -\frac{1}{2}\rho CS\frac{d}{dt}x + F\cos\theta\,, (1)$$

where m is the mass of the BFR, F is thrust, θ is the angle of the wriggling motion, ρ is the density of air, C is the air resistance coefficient, and S is the projected area of the BFR. The thrust F is measured to construct the equation of motion of the BFR.

III. MEASUREMENT SYSTEM

We focused on the thrust of the BFR and measured it with a force sensor. We considered two parameters of the BFR's wriggling motion: the oscillation angle and the oscillation frequency. To determine the equation of motion, we measured the thrust. In addition, the actual robot movements were measured, and the results were compared with those of the thrust measurement experiment. The thrust is corrected because there is a difference in the position of the rotation axis in the real machine and the thrust measurement experiment.

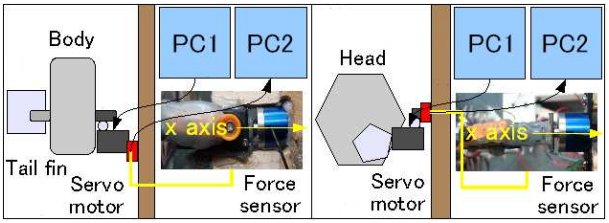

Fig.4. Thrust measurement system

1. Real machine measurements

We measured the propulsion of the BFR experimentally using an actual robot. Fig. 3 shows the real machine measurement system. Four tracking points were set on the BFR, and images were captured as the BFR advanced. The movement of the BFR was measured as two-dimensional coordinates.

2. Thrust measurement

In this study, the thrust of the BFR was measured with a force sensor. Fig. 4 shows the thrust measurement system. The force sensor, the body, and the caudal fin of the BFR were fixed to a wood post (prop), and the force generated by the wriggling motion was measured with the force sensor. Similarly, the movement of the head, which vibrates along with the wriggling motion, was also measured.

3. Thrust correction

There is a difference in the position of the rotation axis in the real machine and in the thrust measurement experiment, as illustrated in Fig. 5. In the thrust measurement experiment, the rotation axis determines the position of the servo motor. In this case, the length of the BFR that contributes to propulsion is the entire length of the BFR. The length of the head is defined as L_1, and the length of the body is defined as L_2.

The rotation axis moves in the actual machine, as shown in Fig. 5. Therefore, the length of the BFR that contributes to propulsion is shorter in both the head and the body. There is a difference in the thrust produced in the real machine and the thrust measurement experiment. In this case, the length of the head that contributes to propulsion is defined as nL_1, and that of the body is defined as mL_2 ($0 < n < 1$, $0 < m < 1$). The numerical values of n and m are the coordinates of the rotation axis in the head and the body where the wriggling motion of the BFR occurs. The two points are the points that exist between two tracking points of the head and the body in the real machine experiment, where the distance moved is minimized.

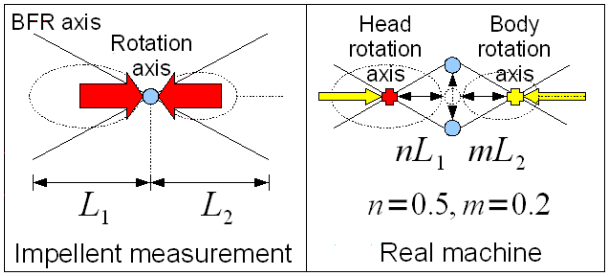

Fig.5. Difference of rotation axis

The numerical values of n and m were calculated from the results of the real machine experiment. The values of n and m were varied from 0.1 to 0.9 in steps of 0.1, and the values that minimized the distance moved were identified. The numerical results are illustrated in Fig. 6. From the results, we defined $n = 0.5$ and $m = 0.2$. Therefore, in the real machine, the length of the head that contributes to propulsion is $0.5L_1$, and that of the body is $0.8L_2$.

In short, because the thrust produced is different in the real machine and the thrust measurement experiment, it is necessary to correct the thrust with the values of n and m.

First, the thrust of the head is corrected. Because $n = 0.5$, the rotation axis of the head is at the center of the head. A positive thrust and a negative thrust cancel each other out in the wriggling motion in one cycle. Therefore, the thrust that the head generates is 0.

Next, the thrust that the body generates is corrected. The thrust is proportional to the volume of air pushed out behind by the wriggling motion. In this case, where $m = 0.2$, the length of the body that contributes to propulsion is $0.8L_2$, and a body length of $0.2L_2$ generates a negative thrust. As a result, the thrust that the body and the caudal fin generate is corrected by a factor of 0.6. In addition, the angle of the wriggling motion is 45 degree, but because the rotation axis and the head move, the angle of the wriggling motion becomes smaller than 45 degree. From the measurement results, the angle of the head was 15 degree, and the angle of the body was 30 degree during the wriggling motion. Therefore, the oscillation angle of the body is assumed to be 30 degree in the thrust measurement experiment.

IV. EXPERIMENT

1. Real machine experiment

Images of the BFR during propulsion were captured with a camera. The wriggling motion of the BFR is oscillating movement having an oscillation angle and

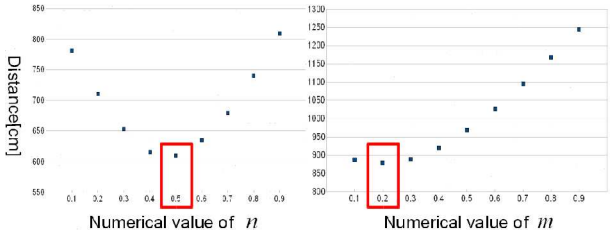

Fig.6. Numerical values of n and m

oscillation speed. In a preliminary study, we found that the velocity of the BFR was highest when the oscillation angle was 45 degrees and increased as the oscillation speed increased. Therefore, we set the following experimental conditions: the oscillation angle was 45 degree, the oscillation frequency was 0.5 Hz, which was the maximum speed of the servo motor, the measurement time was 15 s, and the sampling frequency was 30 fps.

2. Thrust measurement experiment

The thrust of the BFR was measured with the force sensor. We set the experimental conditions according to the thrust correction. The oscillation angle was 30 degree, the oscillation frequency was 0.5 Hz, the measurement time was 15 s, and the sampling frequency was 1024 Hz.

V. RESULTS

The velocity of the BFR was calculated from the results of the real machine experiment and the thrust measurement experiment.

The distance moved by the tracking points on the BFR was measured from the results of the real machine experiment, and the velocity of the BFR was calculated every 0.3 s.

The results of the thrust measurement experiment were substituted into the equation of motion of the BFR, and the velocity of the BFR was calculated. Fig. 7 shows the numerical results. In Fig. 7, the horizontal axis corresponds to time and the vertical axis corresponds to the velocity of the BFR. In the thrust measurement experiment, the velocity of the BFR was calculated using the thrust values before correction and after correction. The bottom graph shows the difference between the results of the real machine experiment and those after thrust correction. In Fig. 7, because the thrust was corrected, the calculated value become close to the velocity of the real machine. As a result, it was possible to construct an equation of motion closer to that of the real machine by considering the movement of the real machine. The maximum velocity of the BFR was about 0.6 m/s for the real machine and the equation of motion,

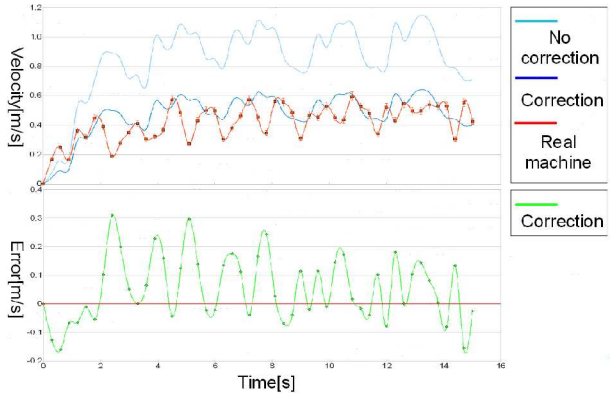

Fig.7. Velocity of the BFR

showing good agreement. However, even after the thrust had been corrected, it was confirmed that the difference in velocity compared with the real machine was about 0.3 m/s at most. Therefore, there must be force that was not taken into account in constructing the equation of motion.

VI. DISCUSSION

There was a difference between the results observed with the real machine and those obtained with the equation of motion. In Fig. 7, the velocity periodically decreases in the calculation results for the real machine.

The cause of this is thought to be the change in the projected area. In this study, the projected area of the BFR was assumed to be constant in calculating the velocity. In practice, however, the projected area changes over time because the head of the BFR moves during the wriggling motion. The reason why the velocity of the real machine decreases is that the projected area increases periodically.

Similarly, it is also necessary to consider the force that the pectoral fins generate during the wriggling motion.

In this research, the velocity of the BFR was calculated for one pattern of wriggling motion; in future, it will be necessary to calculate the velocity for other wriggling motions.

VII. CONCLUSION

The aims of this study were to measure the thrust of the BFR and to construct an equation of motion. We measured the thrust with a force sensor and constructed the equation of motion by comparing the results with those for real machine movement. As a result, it was possible to construct an equation of motion closer to that of the real machine by considering the movement of the real machine.

VIII. FUTURE TASKS

Tasks to be implemented in future work include considering the change in the projected area, conducting experiments using other wriggle motion patterns, repeating the motion experiments for a BFR with pectoral fins, constructing an equation of motion, and controlling the air speed.

ACKNOWLEDGMENTS

A part of this study was supported by the HAYAO NAKAYAMA Foundation for Science & Technology and Culture and a Grant-in-Aid for Scientific Research (Basis Research (C), Assignment Number: 21500511).

REFERENCES

[1] Kazuhiro Hosoi, Masanori Sugimoto, "An Autonomous Security System Using Multi-Flying Robots," The 18th Annual Conference of the Japanese Society for Artificial Intelligence, 2C1-04, 2004.
[2] Junzhi Yu, Lizhong Liu, Long Wang, Min Tan, De Xu, "Turning Control of a Multilink Biomimetic Robotic Fish," IEEE TRANSACTIONS ON ROBOTICS, Vol. 24, No. 1, pp. 201-206, February 2008.
[3] Junzhi Yu, Long Wang, Min Tan, "Geometric Optimization of Relative Link Length for Biomimetic Robotic Fish," IEEE TRANSACTIONS ON ROBOTICS, Vol. 23, No. 2, pp. 382-386, APRIL 2007.
[4] Motomu Nakashima, Kyosuke Ono "Dynamics of Two-Joint Dolphinlike Propulsion Mechanism (1st Report, Analytical Model and Analysis Method)," The Japan Society of Mechanical Engineers, 62-600(B), pp. 3044-3051, 1996.
[5] H. Zhang, J. P. Ostrowski, "Visual Servoing with Dynamics: Control of an Unmanned Blimp," Proc. IEEE Int. Conf. Robotics and Automation, pp. 618-623, 1999.